

## DNA as Invisible Ink for AFM Nanolithography

Jian Liang,<sup>†</sup> Matteo Castronovo,<sup>†,‡</sup> and Giacinto Scoles<sup>\*,†</sup>

<sup>†</sup>Department of Biology, Temple University, 1900 North 12th Street, Philadelphia, Pennsylvania 19122, United States

<sup>‡</sup>Experimental and Clinical Pharmacology Unit, CRO-National Center Institute, Via Franco Gallini 2, I-33081 Aviano Pordenone, Italy

**S** Supporting Information

**ABSTRACT:** We have used nanografting, an atomic force microscopy (AFM)-based nanolithography technique, to fabricate thiolated DNA nanostructures on gold surfaces. The tip-guided assembly offers opportunities for locally controlling the packing order, density, and thus the thickness of the DNA patterns. By selecting proper nanografting parameters, we can embed single-stranded DNA (ssDNA) patches into a background composed of the same DNA molecule prepared by self-assembly, in which the patches remain topographically (and chemically) invisible but have much improved packing order. When the complementary DNA (cDNA) is added, the thickness of the nanografted layer increases much more dramatically than that of the self-assembled layer during the hybridization process, and as a result, the pattern emerges. Interestingly, the pattern can be reversibly hidden and shown with high fidelity simply by dehybridizing and appending the cDNA repeatedly.

Surface-bound DNA molecules have generated tremendous interest because of their potential applications in biosensing and biorecognition,<sup>1,2</sup> for guiding the assembly of nanoparticles,<sup>3,4</sup> in the study of electrical<sup>5,6</sup> and mechanical<sup>7,8</sup> properties of the molecule, and as building blocks of various supramolecular architectures.<sup>9,10</sup> One of the convenient ways to tether DNA chemically onto surfaces is the self-assembly technique. For instance, a thiol linker can be introduced into the DNA molecule, and a self-assembled monolayer (SAM) of such DNAs can readily form on gold surfaces through the sulfur–gold linkage. For more controlled nanoscale DNA patterning, self-assembly can be combined with scanning probe lithography techniques, such as nanografting<sup>11</sup> or dip-pen nanolithography.<sup>12</sup> The major difference between these two techniques is that while dip-pen nanolithography writes on a blank substrate (addition reaction to the surface), nanografting removes the initial molecules in the scanning region and fabricates patterns within an existing matrix monolayer (surface substitution reaction). The matrix can confine the lateral diffusion of the grafted molecules and in particular can serve as a standard reference when its properties are relatively well-known. Tarlov and co-workers<sup>13–15</sup> systematically investigated the structural properties of SAMs of thiol-derivatized DNAs, including their surface density and molecular conformation. The thickness of ssDNA SAMs was found to be significantly less than the contour length or the length of the helix form of the molecule, indicating that the majority of the DNAs are not

in the “standing-up” configuration. Furthermore, longer ssDNA strands are usually in less ordered arrangements and show more polymeric behavior, in contrast to the typical *n*-alkanethiol (containing 8–20 carbons) SAMs, where the molecules are packed parallel to each other. The lack of control of the molecular order hinders the layers from reaching saturation, and the direct correlation between the number of DNA probes and the thickness of the film can be difficult to determine because different molecular orders may result in various film densities (porous or densely packed). In nanografting, on the other hand, the tip-guided self-assembly offers the opportunity of tuning the nanostructure with additional parameters such as the scanning speed and the density of scan lines. It has been demonstrated that nanografted ssDNA layers have various thickness (up to the full length of the molecule) depending on the experimental conditions,<sup>11,16</sup> suggesting that the AFM probe can play an important role in modifying the local structure of the DNA monolayers, including the density and packing order. Additionally, hybridization of the surface-bound ssDNAs with their complements to form double-stranded (ds) helices can further modulate the thickness of the layer because the dsDNA has a stiff, rodlike structure (persistence length of ~50 nm) that has more fixed orientation and is less compressible. Here we show that when nanografting ssDNA patterns into a matrix composed of the same molecule, we can selectively control the thickness of the grafted layer in such a way that the drawing remains topographically (and chemically) invisible. Incubating and dehybridizing the cDNA can make the patterns reversibly emerge and disappear because the nanografted layer undergoes a much more dramatic topographic change than the self-assembled layer during these processes. The ability to use AFM in DNA nanopatterning in a well-addressable and controllable manner reduces the minimum amount of DNA that can be immobilized,<sup>17</sup> which is important because many DNA-based biosensors utilize hybridization in their detection schemes, and consequently, their sensitivity depends decisively on the hybridization efficiency.<sup>18</sup>

To elucidate the difference in the thickness of DNA films prepared by self-assembly and by nanografting, we compared them with bioresistant oligo(ethylene glycol) (OEG) monolayers side-by-side. Experiments performed by different groups have confirmed that *n*-alkanethiol SAMs, whether prepared by self-assembly or nanografting, can serve as reliable height references with molecules in the all-trans conformation.<sup>19,20</sup>

Received: August 14, 2011

Published: December 12, 2011

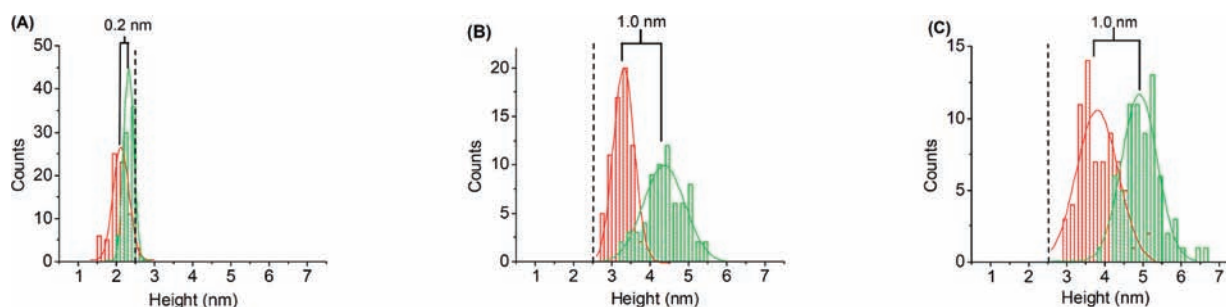


**Figure 1.** Histograms of the thickness of self-assembled ssDNA layers (red bars) as a function of the concentration of the molecule in solution, using nanografted OEG patches as references. The DNA concentrations were (A) 1, (B) 5, and (C) 10  $\mu\text{M}$ . After hybridization (green bars), the peak positions of the Gaussian fits to the histograms (solid lines) increased by (a) 0.2, (b) 1.0, and (c) 1.0 nm. The dashed lines indicate the height of the OEG layer as a reference to guide the eyes.

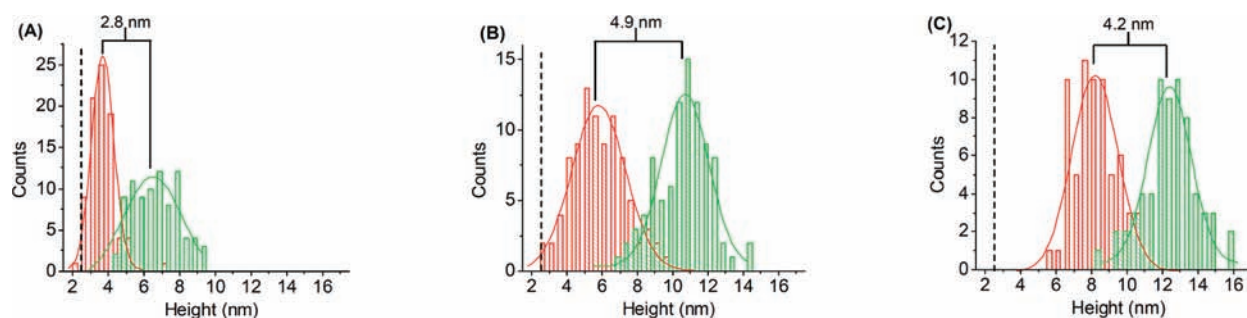


**Figure 2.** Histograms of the thickness of nanografted ssDNA patterns (red bars) as a function of the scan line density, using self-assembled OEG layers as references. The scan line densities were (A)  $1/8$ , (B)  $1/2$ , and (C)  $2 \text{ nm}^{-1}$ . After hybridization (green bars), the peak positions of the Gaussian fits to the histograms (solid lines) increased by (a) 2.8, (b) 4.9, and (c) 4.2 nm. The dashed lines indicate the height of the OEG layer as a reference to guide the eyes. Under the same concentration of ssDNA (5  $\mu\text{M}$ ), the resulting nanografted patterns have a much broader accessible height distribution and better hybridization capability (see Figure 1B).

The OEG-modified thiol  $[\text{HS}(\text{CH}_2)_{11}(\text{OCH}_2\text{CH}_2)_6\text{OH}]$  SAMs in our experiments demonstrated similar behavior. The direct comparison of height, as shown in Figure S1 in the Supporting Information (SI), indicated that OEG layers prepared by self-assembly and by nanografting had the same thickness ( $\sim 2.5$  nm, in agreement with previous reports<sup>21,22</sup>). For DNA layers, however, the thickness of the thin films prepared by self-assembly and by nanografting can be substantially different. Figure 1 shows histograms of the thickness of 44 base pair ssDNA layers prepared by self-assembly, using nanografted patches of OEG as the height reference. To construct the histograms, the topographical image of each patch was recorded, and cross-sectional line profile analysis was carried out to find out the height difference between the pattern and the background (see the SI for more details). The peak positions of Gaussian fits to the histograms were 0.4 nm lower, 0.8 nm higher, and 1.3 nm higher than the OEG film for initial thiolated DNA concentrations of 1, 5, and 10  $\mu\text{M}$ , respectively. Since the OEG layer was  $\sim 2.5$  nm thick, the height of the DNA layers was only  $\sim 2$  nm at low initial concentration (1  $\mu\text{M}$ ), far lower than the full length of the molecules (15–16 nm) but close to the diameter of the DNA helix structure,<sup>23</sup> suggesting that the DNA molecules significantly deviate from the surface normal, in agreement with other reports in the literature such as the one by Jiang and co-workers,<sup>24</sup> who probed DNA SAMs with electron spectroscopy and surface plasmon resonance. Higher concentrations of DNA crowd the surface with more molecules at the initial growing stage, but the increment in thickness was  $< 2$  nm (only  $\sim 15\%$  of the molecular length) when the concentration increased 10-fold from 1 to 10  $\mu\text{M}$ .

Interestingly, further hybridization of the ssDNA into dsDNA did not increase the thickness significantly ( $\sim 1$  nm, less than 10% of the molecular length). On the other hand, DNA nanostructures with variable height are more readily achievable by the application of an AFM tip through nanografting. Figure 2 demonstrates the height histograms for the same DNA layer as in Figure 1 but prepared by nanografting under a fixed concentration of 5  $\mu\text{M}$ . With different scan line densities, the nanografted patterns can be 0–8 nm ( $> 50\%$  of the full length of the DNA) higher than the OEG SAM. More detailed reports about different factors affecting the height of a nanografted DNA pattern have been published elsewhere<sup>16,25</sup> and have shown that even greater height (up to the full length of the ssDNA) can be obtained by selecting the proper scanning parameters, DNA concentration, and solvent. Remarkably, Figure 2 shows that the DNA grew significantly in height ( $> 3$  nm or 20% of the molecular length) during hybridization even when the initial thickness was similar to that prepared by self-assembly (Figures 2A and 1B), indicating a higher hybridization efficiency than for the self-assembled ssDNA layers.

It is important to understand from a molecular perspective the formation of DNA layers prepared by self-assembly and by nanografting for better clarification of the resulting nanostructures. There have been reports in the literature that the density of ssDNA molecules in SAMs increases quickly in the initial stage of self-assembly because of surface adsorption but then reaches saturation after a couple of hours.<sup>13</sup> The saturated density typically ranges between  $10^{12}$  and  $10^{13} \text{ cm}^{-2}$ ,<sup>13,26,27</sup> which cannot be further increased by longer incubation time. These density values are only a fraction of the value of  $\sim 3 \times$

$10^{13} \text{ cm}^{-2}$  expected for DNAs that are closely packed in the helix form with a diameter of  $\sim 2 \text{ nm}$  along the surface normal.<sup>11,14</sup> Moreover, it has often been demonstrated that the thickness of the films is far lower than the full molecular length.<sup>24,28</sup> These results suggest that the DNA SAMs, unlike those made of *n*-alkanethiols, may intrinsically lack packing order. First, the flexibility of the ssDNA chain (persistence length of  $\sim 1 \text{ nm}$ ) and the possibility of forming intrastrand and interstrand hydrogen bonds may lead to entanglement of different segments of the molecule and different molecules. Second, the electrostatic repulsion between the charge-bearing DNA oligomers may prevent them from packing at high densities. Last but not least, some oligonucleotide sequences (e.g., adenine) exhibit rather strong and rapid nonspecific adsorption to the gold surface,<sup>29</sup> which may lead to the horizontal attachment of the molecule.

On the other hand, in nanografting the AFM tip scans the surface (in a solution containing thiolated DNAs) at a relatively high force load (typically  $10^2 \text{ nN}$  depending on the sharpness of the tip). Because of tip-induced mechanical perturbations, the molecules in the matrix SAM locally exchange with the DNA in situ. Immediately after the scanning is complete (typically within a few minutes), a patch is well-formed and ready to be imaged by the AFM under low force. The tip scanning in the adjacent area during the assembly probably removes the possible lying-down adsorption of the DNAs, freeing the gold surface and preparing it to accommodate more molecules, which explains the fact that the thickness of the nanografted patches increases with the density of the scan lines. Additionally, the friction between the tip and the surface during scanning may provide extra thermal energy for overcoming the energy barrier of desorption of the nucleotide bases from the surface. Furthermore, the different increases in height after hybridization (Figures 1 and 2) imply that the local structures of the nanografted layers and thus their ability to hybridize have been modulated by the AFM tip. Although the detailed mechanism of the tip modulation is not completely clear at this stage, the results can be understood as a “combing” effect in which the DNA packing order is improved by high-load scanning, with a definitive effect on the DNA reactivity. Interestingly, a similar effect was also observed in nanografting of dithiol molecules in our previous report,<sup>30</sup> in which the nanografted layers demonstrated much improved smoothness and better control of the molecular stacking in comparison with the ones prepared by self-assembly. The disorder of ssDNA SAMs hinders the hybridization efficiency, so their thickness does not change significantly when the cDNA is introduced.<sup>31</sup> On the other hand, Mirmomtaz et al.<sup>16</sup> pointed out that the hybridization efficiency can be  $>50\%$  for nanografted DNA layers because the molecules are less entangled. As a result, unless the height has already reached saturation, in which case no change can be recognized, the increase in height during hybridization of the nanografted ssDNA patterns is relatively large.

By utilizing the elastic response of ssDNA layers to hybridization, we can use thiolated DNA as an invisible and mechanically activated “ink” for AFM nanolithography. For instance, we can nanograft an ssDNA pattern into a layer made of the same molecule but prepared by self-assembly. By selecting proper self-assembly and nanografting parameters, we can control the height of the patch to be the same as that of the background, so the pattern is initially invisible in the topography image but has a different packing order (Figure

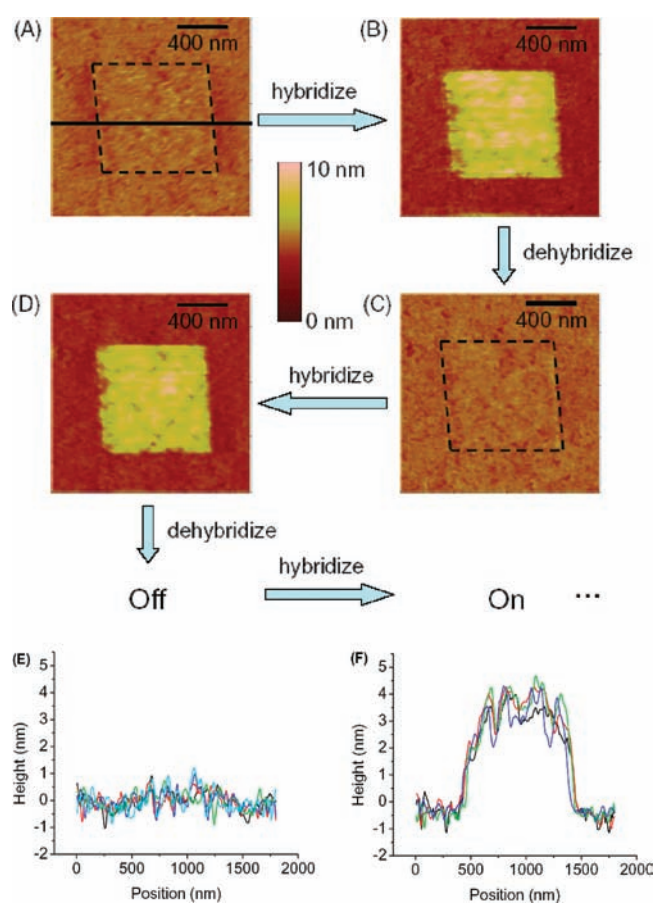


**Figure 3.** DNA as an invisible ink for nanolithography. (A) An ssDNA patch is nanografted in a SAM composed of the same molecule, and the height of the patch is tuned to be the same as its surroundings (“Off” state) by selecting proper nanografting parameters. The dotted line marks the position of the patch as a guide to the eyes. (B) Hybridizing the ssDNA reveals the hidden pattern (“On” state) because of its better packing order and higher hybridization efficiency. (C) Lowering the ionic strength of the solution dehybridizes the dsDNAs, and the pattern disappears. (D) The pattern is restored by introducing the cDNA again in TE buffer. Such hybridization/dehybridization cycles can be repeated multiple times, and the pattern is switched between the “On” and “Off” states. Line profiles across the pattern [as the position of the black line in (A)] show five successive “Off” states (E) and four successive “On” states (F), demonstrating that the height of the pattern is highly conserved through the hybridization/dehybridization cycles.

3A). Because the self-assembled layers have relatively constant height (Figure 1), this thickness matching can be more conveniently achieved by varying the scan line density (and the DNA concentration, if necessary) in nanografting. It is noteworthy that low scan line density is usually preferred because the nanografted layers are generally higher than the self-assembled ones (Figures 1 and 2). In our experiments, we first allowed the ssDNA to self-assemble for 2.5 h under a concentration of  $5 \mu\text{M}$  and then nanografted the patterns with a scan line density of  $1/8 \text{ nm}^{-1}$ , as Figures 1B and 2A show that the histograms of the film thicknesses largely overlap under these two conditions. When the cDNA was subsequently added, the pattern appeared because of its higher hybridization efficiency (Figure 3B). In this way, an initially flat surface covered with the same molecule could be made to display well-defined features upon a relatively simple operation (hybrid-

ization). Interestingly, this hybridization process was completely reversible. One of the important factors for maintaining the stability of the dsDNA helical structure is the ionic strength of the solution. Consequently, incubating the dsDNA with Milli-Q water for several hours caused the the DNA to dehybridize, and the pattern disappeared again (Figure 3C). After that, the pattern could be restored by immersing the sample into Tris-EDTA (TE) buffer containing the cDNA (Figure 3D). When this hybridization/dehybridization process was repeated multiple times, the pattern was reproducibly switched between the two constant "On" and "Off" states (see the line profiles in Figure 3E,F), providing a good example of "writing/reading/erasing", which is rather uncommon in this field.

In conclusion, we have shown the feasibility of using DNA as an invisible ink for AFM nanolithography in a matrix composed of the same molecule (or, in principle, other inert backgrounds). The tip-guided assembly and local scanning can partially eliminate nonspecific adsorption to the surface and molecular entanglement, which probably facilitates the hybridization kinetically. As a result, during the hybridization process the nanografted layer has higher hybridization ability, and the thickness increases much more significantly than that of the self-assembled layer regardless of the initial height. The high fidelity of the height and size of the pattern during the On/Off switching indicates that the structural modification is localized and that diffusion and desorption of the molecules are negligible. This technique offers sufficient encryption possibilities because of the binding specificity between the base pairs, which is supported by the experiment that the existence of non-cDNA has no impact on the thickness of surface-bound ssDNA patterns.<sup>16</sup> Moreover, a variety of physical and chemical methods are readily available for dehybridizing the dsDNA molecules,<sup>32,33</sup> providing flexibility for erasing the codes. Last but not least, when the present approach is combined with other techniques such as DNA stamping,<sup>34</sup> surface-tethered DNA arrays can be fabricated and transfer of the patterns can be realized (see the SI for more details).

## ■ ASSOCIATED CONTENT

### ■ Supporting Information

Experimental procedures, figures showing the thickness of self-assembled and nanografted OEG monolayers, and proposed applications of the technique. This material is available free of charge via the Internet at <http://pubs.acs.org>.

## ■ AUTHOR INFORMATION

### Corresponding Author

[gscoles@princeton.edu](mailto:gscoles@princeton.edu)

## ■ ACKNOWLEDGMENTS

The authors thank Professor Eric Borguet and other members of our lab for helpful discussions. The College of Science and Technology and the Department of Biology of Temple University are gratefully acknowledged for their financial support.

## ■ REFERENCES

- (1) Du, H.; Disney, M. D.; Miller, B. L.; Krauss, T. D. *J. Am. Chem. Soc.* **2003**, *125*, 4012.
- (2) De, M.; Ghosh, P. S.; Rotello, V. M. *Adv. Mater.* **2008**, *20*, 4225.
- (3) Dillenback, L. M.; Goodrich, G. P.; Keating, C. D. *Nano Lett.* **2006**, *6*, 16.

- (4) Jackobsen, U.; Simonsen, A. C.; Vogel, S. *J. Am. Chem. Soc.* **2008**, *130*, 10462.
- (5) Porath, D.; Bezryadin, A.; de Vries, S.; Dekker, C. *Nature* **2000**, *403*, 635.
- (6) Xu, B. Q.; Zhang, P. M.; Li, X. L.; Tao, N. J. *Nano Lett.* **2004**, *4*, 1105.
- (7) Bustamante, C.; Bryant, Z.; Smith, S. B. *Nature* **2003**, *421*, 423.
- (8) Albrecht, C.; Blank, K.; Lalic-Multhaler, M.; Hirler, S.; Mai, T.; Gilbert, I.; Schiffmann, S.; Bayer, T.; Clausen-Schaumann, H.; Gaub, H. E. *Science* **2003**, *301*, 367.
- (9) Willner, I.; Willner, B. *Nano Lett.* **2010**, *10*, 3805.
- (10) Karl, B.; Wiberg, J.; El-Sagheer, A. H.; Ljungdahl, T.; Martensson, J.; Brown, T.; Norden, B.; Albinsson, B. *ACS Nano* **2010**, *4*, 5037.
- (11) Liu, M. Z.; Amro, N. A.; Chow, C. S.; Liu, G. Y. *Nano Lett.* **2002**, *2*, 863.
- (12) Demers, L. M.; Ginger, D. S.; Park, S. J.; Li, Z.; Chung, S. W.; Mirkin, C. A. *Science* **2002**, *296*, 1836.
- (13) Herne, T. M.; Tarlov, M. J. *J. Am. Chem. Soc.* **1997**, *119*, 8916.
- (14) Steel, A. B.; Levicky, R. L.; Herne, T. M.; Tarlov, M. J. *Biophys. J.* **2000**, *79*, 975.
- (15) Petrovykh, D. Y.; Kimura-Suda, H.; Tarlov, M. J.; Whitman, L. J. *Langmuir* **2004**, *20*, 429.
- (16) Mirmomtaz, E.; Castronovo, M.; Grunwald, C.; Bano, F.; Scaini, D.; Ensafi, A. A.; Scoles, G.; Casalis, L. *Nano Lett.* **2008**, *8*, 4134.
- (17) Zhou, D.; Sinniah, K.; Abell, C.; Rayment, T. *Angew. Chem., Int. Ed.* **2003**, *42*, 4934.
- (18) Rosi, N. L.; Mirkin, C. A. *Chem. Rev.* **2005**, *105*, 1547.
- (19) Liu, G. Y.; Xu, S.; Qian, Y. L. *Acc. Chem. Res.* **2000**, *33*, 457 and references therein.
- (20) Liang, J.; Scoles, G. *Langmuir* **2007**, *23*, 6142.
- (21) Harder, P.; Grunze, M.; Dahint, R.; Whitesides, G. M.; Laibinis, P. E. *J. Phys. Chem. B* **1998**, *102*, 426.
- (22) Hu, Y. Ph.D. Thesis, Princeton University, Princeton, NJ, 2005.
- (23) Berg, J. M.; Tymoczko, J. L.; Stryer, L. *Biochemistry*, 5th ed.; Freeman: New York, 2002.
- (24) Boozer, C.; Chen, S.; Jiang, S. *Langmuir* **2006**, *22*, 4694.
- (25) Liu, M.; Liu, G. Y. *Langmuir* **2005**, *21*, 1972.
- (26) Steel, A. B.; Herne, T. M.; Tarlov, M. J. *Anal. Chem.* **1998**, *70*, 4670.
- (27) Peterlinz, K. A.; Georgiadis, R. M.; Herne, T. M.; Tarlov, M. J. *J. Am. Chem. Soc.* **1997**, *119*, 3401.
- (28) Cho, Y.-K.; Kim, S.; Lim, G.; Granick, S. *Langmuir* **2001**, *17*, 7732.
- (29) Wolf, L. K.; Gao, Y.; Georgiadis, R. M. *Langmuir* **2004**, *20*, 3357.
- (30) Liang, J.; Rosa, L. G.; Scoles, G. *J. Phys. Chem. C* **2007**, *111*, 17275.
- (31) Peterson, A. W.; Heaton, R. J.; Georgiadis, R. M. *Nucleic Acids Res.* **2001**, *29*, 5163.
- (32) Nasef, H.; Ozalp, V. C.; Beni, V.; O'Sullivan, C. K. *Anal. Biochem.* **2010**, *406*, 34.
- (33) Zhang, N. B.; Mitirovski, S. M.; Nuzzo, R. G. *Anal. Chem.* **2007**, *79*, 9014.
- (34) Yu, A. A.; Saves, T.; Cabrini, S.; DiFabrizio, E.; Smith, H. I.; Stellacci, F. *J. Am. Chem. Soc.* **2005**, *127*, 16774.